



HAL
open science

Chemical ozone loss and chlorine activation in the Antarctic winters 2013–2020

Raina Roy, Pankaj Kumar, Jayanarayanan Kuttippurath, Franck Lefèvre

► **To cite this version:**

Raina Roy, Pankaj Kumar, Jayanarayanan Kuttippurath, Franck Lefèvre. Chemical ozone loss and chlorine activation in the Antarctic winters 2013–2020. *Atmospheric Chemistry and Physics Discussions*, 2024, 10.5194/egusphere-2023-1189 . insu-04146286

HAL Id: insu-04146286

<https://insu.hal.science/insu-04146286>

Submitted on 29 Jun 2023

HAL is a multi-disciplinary open access archive for the deposit and dissemination of scientific research documents, whether they are published or not. The documents may come from teaching and research institutions in France or abroad, or from public or private research centers.

L'archive ouverte pluridisciplinaire **HAL**, est destinée au dépôt et à la diffusion de documents scientifiques de niveau recherche, publiés ou non, émanant des établissements d'enseignement et de recherche français ou étrangers, des laboratoires publics ou privés.



1 **Chemical ozone loss and chlorine activation in the Antarctic winters** 2 **2013–2020**

3
4 Raina Roy^{1,2}, Pankaj Kumar¹, Jayanarayanan Kuttippurath¹, Franck Lefevre³

5
6 ¹*CORAL, Indian Institute of Technology Kharagpur, Kharagpur–721302, India.*

7 ²*Department of Physical Oceanography, Cochin University of Science and Technology, Kochi, India.*

8 ³*LATMOS/IPSL, Sorbonne Université, UVSQ, CNRS, Paris, France*

9
10 *Correspondence to:* Raina Roy (rainaroy2105@gmail.com)

11 **ABSTRACT**

12
13 Since its discovery in 1985, the formation of ozone holes in the Antarctic and the resulting ultra-violet (UV)
14 radiation reaching the planet's surface has been a source of major concern. The annual formation of ozone hole in
15 the austral springs has regional and global climate implications. Ozone depletion episodes can change precipitation,
16 temperature, and atmospheric circulation patterns, affecting the surface climate primarily in the southern
17 hemisphere (SH). Therefore, the study of ozone loss variability is important to assess its consequential effects on
18 the climate and public health. Our study examines and quantifies the ozone loss and its cycle for the past 8 years
19 in the Antarctic using satellite measurements (Microwave Limb Sounder on Aura). We observe the highest ozone
20 loss (3.8–4.0 ppmv) in spring 2020 followed by 2016. The high chlorine activation (2.3 ppbv), stable polar vortex
21 and extensive areas of polar stratospheric clouds (PSCs) (12.6 Million Km²) favored the large ozone loss in 2000.
22 The spring of 2019 also witnessed a moderately high ozone loss, although the year was marked by a rare minor
23 warming in mid-September. Relatively smaller ozone loss (2.4–2.5 ppmv) was present in 2017 and 2015. It was
24 mainly due to reduced chlorine activation and relatively higher temperature in these winters. Additionally, the
25 chlorine activation in 2015 (1.95 ppbv) was the lowest and the wave forcing from the lower latitudes was very high
26 in 2017 (up to -60 Kms⁻¹). The analysis shows significant interannual variability in the Antarctic ozone as for the
27 immediate previous decade. The study helps to understand the role of the dynamics and chemistry in the inter-
28 annual variability of ozone depletion for the years.

29
30 **Keywords:** Antarctica; Ozone loss estimates; Polar Vortex; climate Change; Model simulations

31 **Short title:** Antarctic ozone loss in 2013–2020



32 INTRODUCTION

33

34 An important event in the Antarctic stratosphere during the austral spring that has caught global attention ever since
35 its discovery in the 1980s is the Antarctic ozone hole (Farman et al., 1985). The chlorine free-radicals released
36 from the chlorofluorocarbons (CFCs) and other ozone-depleting substances (ODSs) activate the catalytic cycles
37 that led to severe ozone loss (e.g. Stolarski and Cicerone, 1974; Rowland et al., 1976). The extreme cold conditions
38 that prevail in the poles facilitate the formation of Polar Stratospheric Clouds (PSCs), which serve as the activation
39 surface for the ODSs. Apart from these, the relatively stable Antarctic polar vortex also contributes significantly to
40 the formation of ozone holes annually (Solomon et al., 2014). Since the discovery of ODSs in the 1970s from
41 anthropogenic activities, the ozone loss continued to rise and reached its worst phase in the late 1980s and early
42 1990s (WMO, 2014; Kuttippurath et al., 2015). The growth in the ODSs was curtailed after the enactment of the
43 Montreal Protocol in 1987. Ratifying of the environmental treaty led to a stabilisation of the loss from the late
44 1990s to the early 2000s in the Antarctic. Despite this, there was no significant increase in total column ozone
45 during those times (e.g. Weatherhead et al., 2000; WMO, 2007; Angell et al., 2009). Beyond 2000, significant
46 recovery trends in the ozone were presented with evidence from both ground or satellite observations (e.g. Yang et
47 al., 2008; Salby et al., 2011; Solomon et al., 2016; Chipperfield et al., 2017; Kuttippurath and Nair, 2017; de Laat
48 et al., 2017; Pazmiño et al., 2018; Wespes et al., 2019). A reduction in the saturation of ozone loss over the period
49 2001–2017 was also observed in the Antarctic and thus confirming the positive ozone trends in the region
50 (Kuttippurath et al., 2018).

51 The rate of ozone loss in the Antarctic is ascertained by a combination of both polar vortex dynamics and chemistry
52 of the winters. Analyses performed by Nedoluha et al. (2016); Strahan et al. (2014); and Strahan et al. (2018)
53 confirmed the importance of chlorine concentration for the formation of ozone holes. They observed a significant
54 reduction in the amount of chlorine free radicals in the twenty-first century and thus, a consistent increase in the
55 corresponding ozone concentration. On the contrary, the longer lifetimes of ODSs (SPARC, 2016), the non-
56 compliance to the protocol and the recent emissions of the ODSs such as CFC-11, brominated ODSs and several
57 other short-lived ODSs (e.g. Maione et al., 2014; Rigby et al., 2017; Montzka et al., 2018; Dhomse et al., 2019),
58 and the increasing emissions of nitrogen oxides (e.g. Butler et al., 2016; Maliniemi et al., 2021) all of which
59 subsequently decelerated the recovery rate of ozone. An evident manifestation of the influence of dynamic
60 variability in the Antarctic polar vortex is found in the years such as 2000, 2002 and 2004 (Langematz and Kunze,
61 2006). Thus, the polar vortex variability is an important factor that controls the rate of ozone depletion (e.g.



62 Stolarski et al., 2006; Zhang et al., 2017). Therefore, a combined action of vortex dynamics and stratospheric
63 chemistry can only lead to significant changes in the Antarctic ozone concentration. The study of annual ozone loss
64 is important as the changes in ozone directly and indirectly affect the climate of southern hemisphere (SH),
65 precipitation patterns, and the circulation in austral summer (e.g. Polvani et al., 2011; Bandoro et al., 2014; Damiani
66 et al., 2020)

67 Here, we present the long-term analysis of ozone loss for the winters 2013–2020 considering the chemical and
68 dynamical characteristics of the periods prior to and of peak ozone loss. Although a few of the years have been
69 studied individually, the long-term analysis helps in better understanding the evolution of the springs/winters
70 (e.g. WMO, 2015; Krummel et al., 2016; Wargan et al., 2020; Klekociuk et al., 2021). The dynamics of these
71 winters are studied using different meteorological parameters. The study offers a high-resolution analysis of the
72 interannual variability of ozone loss at various altitudes using the data obtained from the AURA microwave Limb
73 Sounder (MLS) (Froidevaux et al., 2008; Santee et al., 2008b). The ozone loss is calculated using the passive tracer
74 simulated by the REPROBUS (Reactive Processes Ruling the Ozone Budget in the Stratosphere) chemical transport
75 model (CTM) (Lefèvre et al., 1994). Therefore, we use a single data set and the same method to estimate ozone
76 loss for all eight years to assess the interannual variability, which would make the comparisons among the winters
77 and assessment of polar winters meaningful and coherent.

78 **DATA AND METHODS**

79

80 We have analysed the meteorology of the winters from 2013 to 2020 using the Modern-Era Retrospective analysis
81 for Research and Applications (MERRA-2) data (Gelaro et al., 2017). The MERRA 2 data are available for 42
82 pressure levels with a spatial resolution of $0.5^\circ \times 0.625^\circ$. The nature of austral springs is studied by the examination
83 of four parameters such as the polar cap temperature, zonally averaged from 60° to 90°S at 100 hPa, the minimum
84 polar cap temperature at 10 hPa, the area of polar stratospheric clouds at 460 K, and the mean heat flux averaged
85 from 45° to 75°S . Besides, the MERRA 2 dataset is also employed to analyse the vertical evolution of temperature
86 averaged from 60° to 90°S .

87 We calculate the ozone loss using the REPROBUS model simulations. The model simulates a passive tracer
88 identical to ozone to estimate the loss in each year. It is a three-dimensional model driven by the European Centre
89 for Medium-Range Weather Forecasts (ECMWF) operational analyses. The analysis is performed over the altitude
90 range 1000 to 0.01 hPa (130 levels) (Dee et al., 2011). In the model, the advection is performed by the winds on



91 the hybrid sigma pressure coordinates and the trace gases are advected by a semi-lagrangian technique (Williamson
92 and Rasch, 1989). For our study, the passive tracer identical to the ozone was initialized on July 1 of each year and
93 continued until the end of November. Then the loss is computed by subtracting the measured ozone from the
94 modelled passive tracer. The loss in each day is estimated inside the polar vortex as it is more prevalent there and
95 thus, the polar vortex edge is calculated using the equivalent latitude (Nash et al., 1996; Müller et al., 2005).

96 The ozone and the chlorine monoxide data are taken from the AURA microwave limb sounder (MLS). The MLS
97 data of version 4.2 is used. The data have a vertical resolution of 2–3 km, a vertical range of 261–0.02 hPa and an
98 accuracy of 0.1–0.4 ppmv. Along with this, the ClO measurements are obtained at 640 GHz and are about 3–3.5
99 km over 147–1 hPa, and the accuracy of measurements is about 0.2–0.4 ppbv. These measurements have a latitude-
100 dependent bias of around 0.2–0.4 ppbv, depending on vertical height (Livesay et al., 2013).

101 **RESULTS AND DISCUSSION**

102

103 **Meteorology of the winters**

104

105 Figure 1 shows the meteorology of the winters as illustrated, with the polar cap temperature (60–90°S) at 100 hPa,
106 minimum temperature averaged at 50°–90° S at 100 hPa, PSC area (460 K) and mean heat flux from 45° to 75°S
107 at 100 hPa. The first panel shows the mean temperature (60°–90°S) at 100 hPa, the different coloured lines represent
108 individual years. The lowest temperature for all the years is observed during August. The temperature begins to
109 decrease since the beginning of winter (June) and reaches the lowest in August. It is observed from Fig. 1 that all
110 the years have a temperature in the order of 195–208 K during this period. In the years 2013, 2014, 2015 and 2020
111 the temperature reduces below 195 K (PSC formation threshold) for a short while in August. However, the
112 temperature in 2019 shows a sudden rise from late August (202 K) to mid-September (218 K), indicative of the
113 occurrence of a Sudden Stratospheric Warming (SSW) event. This event has been reported in many of the previous
114 studies and has been described as a minor Warming (mW) (e.g. Shen et al., 2020a,b; Yamazaki et al., 2020). The
115 temperature in August 2017 is also seen to be higher than the other years but lower than that in 2019. There is a
116 visible rise in temperature in the beginning of austral spring. However, temperatures persist below 195 K during
117 early September in 2015. The lowest temperature range during the spring-winter is present in 2015. The
118 temperatures in 2020 also follow this range closely, as depicted in Fig 1.



119 Second panel of Fig 1 shows the minimum temperature during the day averaged in the latitudes surrounding the
120 polar cap. The minimum temperature for all the winters is found to be lower than the PSC formation threshold.
121 This continues for the early spring for all the years except 2019 and the minimum value rises soon after and is
122 higher than 195 K in late spring. The minimum temperature reached their lowest during the day for most days
123 during the spring and winter of 2015, 2018 and 2020. Thus, ideal conditions for the formation of PSCs are found
124 for the majority of winter and spring in all 8 years. Therefore, the PSC area grows since the beginning of austral
125 winter and is observed to be the highest in August (up to 28 million Km²). Corresponding to the periods of longest
126 minimum temperature, the PSCs are estimated to persist until early November in 2015, 2018 and 2020, but are
127 short-lived in 2017 and 2019. As the mean temperature peaks in early to mid-September in 2019, the PSC area
128 drops and diminishes by late September. They dissipated by mid-October in 2017.

129 A major factor affecting the strength of the polar vortex is the tropospheric forcing. The strength of these forcings
130 is highly reduced in the Antarctic except for a few winters. In the study of Zuev et al. (2019), the strengthening of
131 the Antarctic polar vortex in winter and spring is due to the seasonal temperature variations in the subtropical lower
132 stratosphere. The last panel of Fig 1 shows the tropospheric forcing for the years. The heat flux forcings averaged
133 between the adjacent mid-latitude and higher latitudes is found to be directed southwards particularly in late winter
134 and early spring. The years 2019 and 2017 are characterised by very wave forcings, as shown by the flux (from -
135 40 to -50 Kms⁻¹) in the figure. The study conducted by Klekociuk et al. (2020) reported that the easterly phase of
136 QBO in 2017 also favoured the influence of enhanced wave activity on the polar vortex. The studies of Milinevsky
137 et al. (2019) and Evtushevsky et al. (2020) also imply similar results about both winters. The zonal average of heat
138 flux stays between -30 Kms⁻¹ and 10 Kms⁻¹ for much of the winter and the flux increases as the spring approaches.
139 The magnitude of these forcings is limited for the years 2015 and 2020.

140 **Temporal evolution of temperature with altitude**

141 Figure 2 represents the temporal evolution of zonal mean (60°–90°S) temperature profile in the Antarctic for the
142 years 2013–2020. The coloured contours show the growth of temperature across the seasons. The white contour
143 lines represent 188, 195 and 210 K. The zonal winds (westerlies) are overlaid in the figure using the black contour
144 lines and the easterlies are shown in red. The higher temperature contours descend to the lower stratosphere towards
145 the end of austral spring. From the analysis, we observe that the descent to the lower stratosphere is maximum in
146 2019 during mid-September as a consequence of the minor warming. The temperature contours in the range 250–
147 265 K extend to slightly below 10 hPa. We also notice a slight reduction in the speed of westerlies during the



148 period. The zonal mean temperature contours reveal that temperatures below 195 K are found in the lower
149 stratosphere (100–70 hPa) until mid-October in 2015 and 2020. This implies that the temperature conditions during
150 these years are the most ideal for the highest ozone loss. Similarly, the area covered by 195 K is also moderately
151 high in 2013, 2014, 2016 and 2018. However, this is lowest in 2019 and is minimal in 2017. The appearance of
152 easterlies below the 10 hPa altitude is late in 2015 (late November) whereas in 2019 and 2017 the easterlies appear
153 as early as late October. Thus, the vortex lasted the longest in 2015.

154 **Temporal evolution of ozone**

155
156 Figure 3 shows the temporal evolution of ozone (in ppmv) from MLS data for the period 2013–2020. It is observed
157 from previous studies that the ozone loss is maximum in the lower stratosphere in all years (Solomon et al., 1990).
158 The ozone concentration reduces in the lower altitudes every year as time progresses (mainly in spring), as
159 illustrated in Fig 3. Opposed to this, the concentration of ozone in the upper stratosphere increases as time evolves.
160 The ozone concentration in the years 2013, 2014, 2015, 2016, 2018 and 2020 in the lower altitudes (400–600 K) is
161 around 0–3 ppmv. Unlike in the cold winters/springs, the concentration of ozone is slightly higher (1.5–2.5 ppmv)
162 in the same altitude range in 2019. Similarly, in 2017, the ozone concentration in the lower stratosphere is higher
163 than the previous cold years owing to the higher temperature present in the stratosphere. The lowest ozone
164 concentration for the altitude range 400–475 K is observed during the years 2018 and 2020. The 0.5 ppmv contour
165 extends to a level of 475–500 K in both years.

167 **Chlorine activation and ozone loss in 2013–2019.**

168
169 Figure 4 presents the temporal evolution of ClO (right) and ozone loss (left) at different altitudes during the period
170 of study. The ozone loss is highest in the altitude range 400–550 K or in the lower stratosphere for all years and is
171 observed in September and October. The loss is less than 1.4 ppmv in the upper stratosphere in all years. The ozone
172 loss in 2014 and 2015 are almost similar, at about 2.6–3.0 ppmv in the peak ozone loss altitude during September
173 and October. The ozone loss in 2013 reaches up to 3.2 ppmv in mid-October and is higher than that in 2014 and
174 2015 (Vargin et al., 2020). The ozone loss reported in Strahan et al. (2018) for 2015 is similar to the very cold
175 winters in Antarctica and is slightly higher than that found in our study. The preconditioning for ozone loss in 2013
176 and 2014 is ensured by the high chlorine activation at the same altitude range (Kuttippurath et al., 2015). Among
177 the three years prior to the period of the highest ozone loss, the chlorine activation reaches the maximum values in



178 August and September. The chlorine monoxide concentration is found to reach up to 2.2 ppbv in 2013 and 2014,
179 and 2.0 ppbv in 2015. This high chlorine activation remains for almost a month in the peak ozone loss altitude in
180 2013 and for lesser duration in 2014 and 2015. The austral springs of 2017 and 2018 also show similar value ranges
181 for ozone loss, and the chlorine activation in the order of 1.8–2.2 ppbv last for a period of 15–20 days before
182 attaining the maximum ozone loss.

183 We observe the ozone loss in spring 2016 to be about 3–3.2 ppmv in September and 3.4 ppmv in October. It is also
184 noticed that the ozone hole, the PSC occurrences, and chlorine activation (more than a month, up to 2.2 ppbv)
185 lasted longer for the year. An extensive ozone hole is found in 2019 and it lasts from late August to mid-November.
186 The ozone loss has exceeded up to 3.6 ppmv since late September. However, the ozone concentration enhanced
187 after the warming and thus the ozone hole size reduced drastically (Fig 3). The chlorine activation is continuous
188 from August to September (above 2.2 ppbv). The ozone loss values in 2019 and 2020 austral spring are observed
189 to be much higher than the other years. Despite the episode of minor warming in 2019 (3.0–3.6 ppmv), the ozone
190 loss was similar to that in 2016. The nature of the spring was similar to previous warm Antarctic years 1988 and
191 2002. The vortex was short-lived and was highly variable due to increased tropospheric forcing during the year.
192 The ozone loss in 2019 spring was about 3.6 ppmv, which is higher than 2018 ozone loss during the same period
193 (Wargan et al., 2020; Roy et al., 2022). The chlorine activation remained at the peak value (2.0–2.2 ppbv) for
194 several days in August prior to high ozone loss and the spatial distribution (450–550 K) of these high values were
195 the highest compared to all other years. The 2020 ozone loss was very high (up to 4.6 ppmv) and exceeded the
196 maximum ozone loss in 2016. The chlorine activation rose remarkably in the early austral spring (September) (2.0–
197 2.2 ppbv) and is observed to be similar to that in 2016 during this period. Despite the nominal values of chlorine
198 activation in the 2020 spring, the record values of ozone loss may have resulted from the increased aerosol loading
199 into the Antarctic atmosphere from the Australian bushfires in 2020 (e.g. Stone et al., 2021).

200 201 **Interannual variability of ozone loss for the period 2013–2020.**

202
203 The interannual variability of ozone loss and chlorine activation are shown in Figure 5. The ozone loss is computed
204 by taking the mean ozone loss (in ppmv) in the altitude range 450–550 K (the peak ozone loss altitudes) for the day
205 270 to day 300 day (the peak ozone loss period). Similarly, the chlorine activation (in ppbv) is also estimated as a
206 mean of the ClO values over the altitude range (450–550 K) for the day 210 to day 270. The weighted mean of



207 PSC area is also shown in the figure in black solid line for the years 2013–2020. It is observed that the lowest ozone
208 loss is estimated for the years 2015 and 2017 as a result of the minimal chlorine activation prior to the events. The
209 mean ozone loss is 2.4–2.5 ppmv for both the years and the chlorine activation is about 1.95 ppbv (2015) and 2.15
210 ppbv (2017). However, the PSC area in 2015 (11.9 million Km²) was higher than most of the other cold winters.
211 Despite the favourable conditions, the low ozone loss was perhaps associated with the relatively weaker chlorine
212 activation. In the study of Tully et al. (2020), the ozone hole metrics of 2015 is identified to be one of the most
213 severe and extreme opposed to our results, however, this offset is caused by the difference in the period of
214 estimation. They have estimated the values of integrated column deficit and ozone hole area metrics for the period
215 October-December for the corresponding years.

216
217 The PSC area in 2017 (10.2 million Km²) was lower compared to this. The lower value of ozone loss in 2017 spring
218 is also agreed upon in the analysis conducted by Baarthen (2018). Consistent with the results from the column
219 ozone loss analysis the highest ozone loss is estimated to be in 2020 (3.8 ppmv) spring followed by 2016 (3 ppmv).
220 The chlorine activation for both years is also higher than a few other cold winters i.e., 2.2 ppbv in 2016 and 2.3
221 ppbv in 2020. The high ozone loss in 2020 is favoured by the very large PSC area (12.6 million Km²). The 2018
222 spring was also unique in comparison to the other years of study as a consequence of the high chlorine activation
223 (2.3 ppbv) and very high PSC area (12.0 million Km²). The chlorine activation was the highest in 2019 (2.35 ppbv),
224 however, the relatively lower ozone loss in the year is observed to be a direct consequence of the unfavourable
225 dynamic condition (mW). The PSC area is estimated to be the lowest in 2019 (9.4 million Km²). The ozone loss in
226 2013 and 2014 were almost similar (2.7–2.8 ppmv) and the chlorine activation is in the order of 2.2 and 2.25 ppbv
227 in 2013 and 2014, respectively.

228
229

230 **CONCLUSION**

231 A major threat that has plagued humanity since its discovery in the early 1980s is the Antarctic ozone hole and its
232 consequential effects. The ultraviolet (UV) radiation reaching the surface of earth because of the ozone layer
233 destruction can impact humans and other life forms severely. The effectiveness of Montreal Protocol to control the
234 emission of these ODSs thus helped in reverting tremendous damage to the life forms on the planet. In addition to
235 this, ODSs can also cause substantial global warming (Wigley, 1988). Henceforth, a check on their release also
236 helped in reducing the potential global warming and also on regional climate change. Therefore, the study of



237 interannual ozone variability is important to understand the ozone related changes in the surface climate. Here, we
238 assess the ozone loss for an 8-year period (2013–2020) in the Antarctic.

239 The year 2019 had a warm winter with a mW in mid-September. The winter 2017 also showed similar
240 characteristics i.e, there was a sudden increase in temperature during late August, the minimum temperature (about
241 205 K) was also higher in August than that in other years, and the PSC area showed a sharp decrease towards the
242 end of September in that year. The heat flux magnitude for the year (2017) was also higher than the other winters
243 (up to -60 Kms^{-1}). Conversely, the wave fluxes were the lowest in 2015 winter. The temperature and PSC area
244 follow similar temporal evolution in 2013, 2014, 2015, 2016 and 2018. The winter 2020 exhibits a unique
245 meteorology with a long-lasting occurrence of vortex wide PSCs (12.6 million Km^2) and has the highest ozone loss
246 (3.8-4.0 ppmv). The lowest ozone loss (2.4–2.5 ppmv) was estimated in 2015. We observed a minimal ozone loss
247 in 2017 and the loss stayed lesser than 2.8 ppmv for most of October and September. Chlorine activation was also
248 below 1.6–1.8 ppbv in August and September for the year. The study, thus, helps in understanding how the chlorine
249 activation and meteorology of the years influenced the variability of ozone during the period. It is also observed
250 that the dynamics and chemistry of the years played their respective roles in the ozone loss process. The winter
251 2019 is an example of favourable chemistry helping in increased ozone loss though the dynamical conditions were
252 unfavourable.

253 **Acknowledgements**

254 We thank the Indian Institute of Technology Kharagpur, for facilitating the study. We acknowledge free use of the
255 MLS data, which are taken from <https://disc.gsfc.nasa.gov/>. The meteorological data are acquired through
256 <https://ozonewatch.gsfc.nasa.gov>. The REPROBUS data are acquired through IPSL, <http://cds-espri.ipsl.fr/>. We
257 thank Cathy Boone for her help with the model runs, analyses and data transfer, and IPSL for hosting the data.

258 **Data availability**

259 The data used in this study are publicly available. The analysed data/codes can also be provided on request.

260 **Competing Interests**

261 Jayanarayanan Kuttippurath is a member of the editorial board of Atmospheric Chemistry and Physics.

262



263 **Author Contributions**

264 JK conceived the idea, and JK and RR wrote the original manuscript. The manuscript was subsequently revised
265 with inputs from PK and FL. The model runs and model results were analyzed by FL. The data analyses and figures
266 made by RR and PK. All authors participated in discussions and made suggestions, which were considered for the
267 final draft.

268

269

270

271

272

273

274

275

276

277

278

279

280

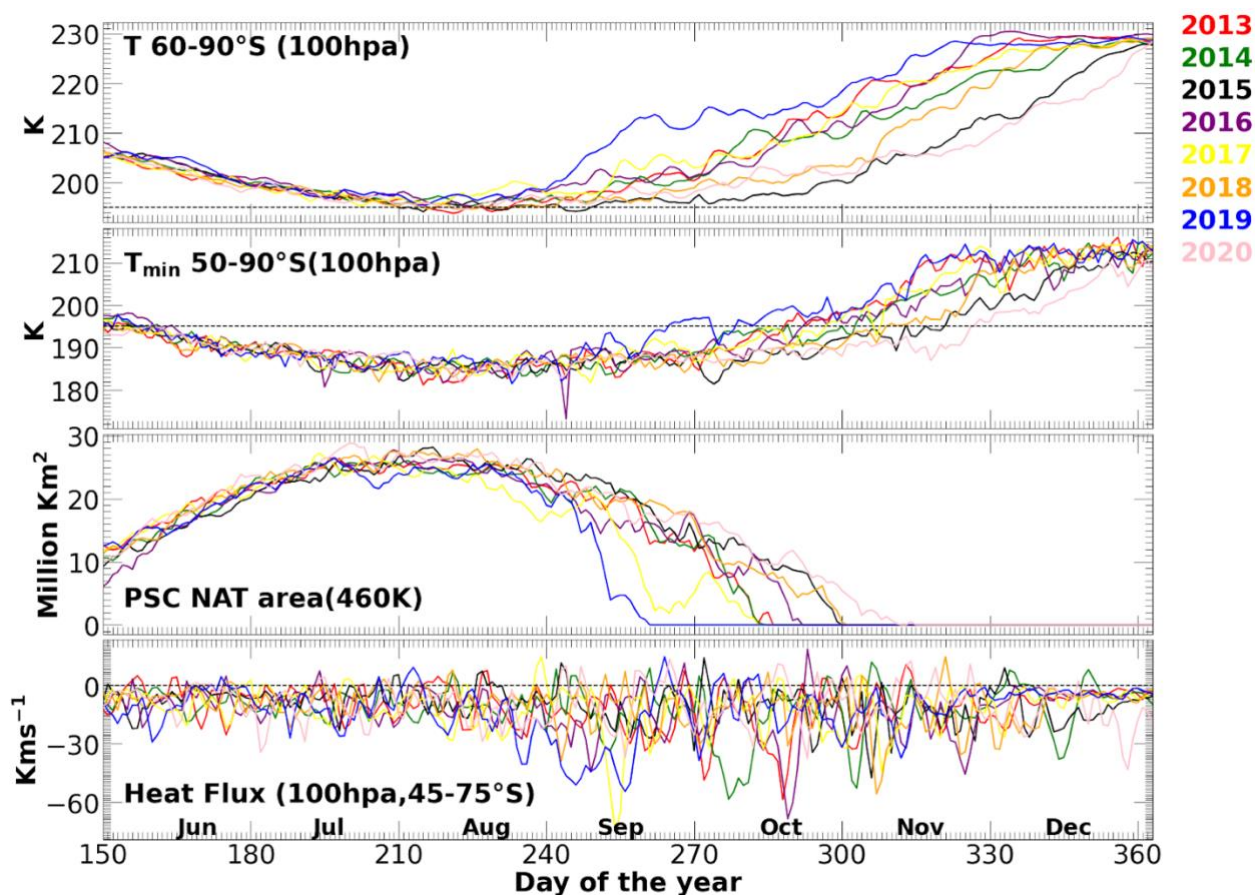
281

282

283

284

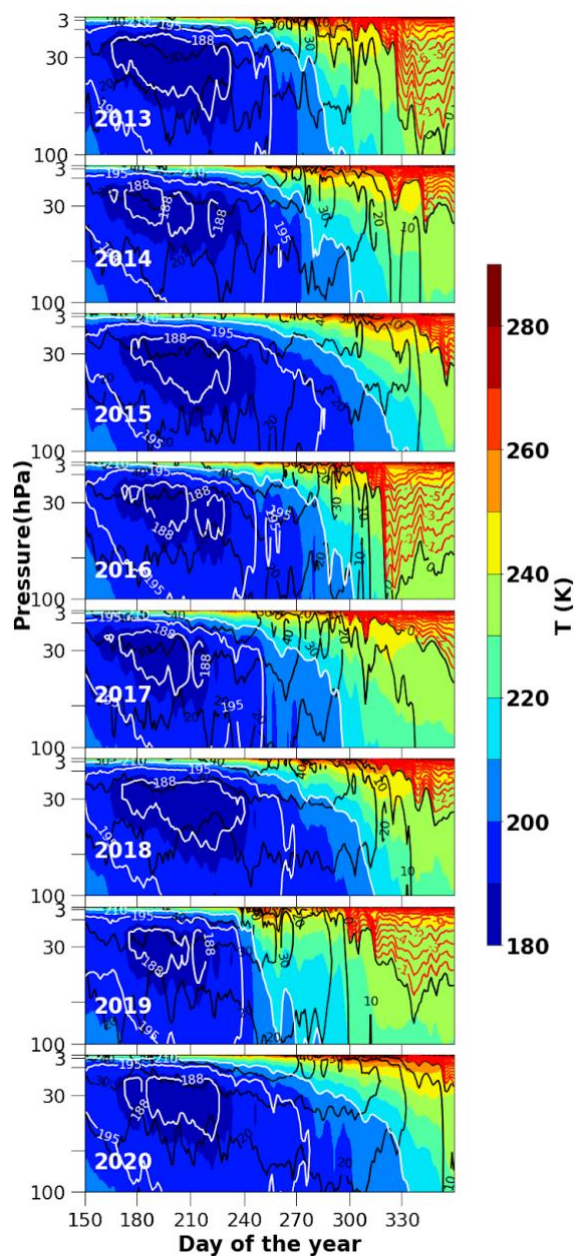
285



286
287

288 **Figure 1:** Meteorology of the years (2013–2020). First panel shows the zonal average temperature (60° – 90° S) at
289 100 hPa. Second panel (from top) shows the minimum temperature at 100 hPa. The black line in the panels show
290 195 K (PSC formation threshold). Third panel (from top) shows the PSC area at 460 K and the bottom panel shows
291 the mean heat flux (45° – 75° S) at 100 hPa. The black horizontal line in the bottom panel shows zero heat flux.

292



293

294

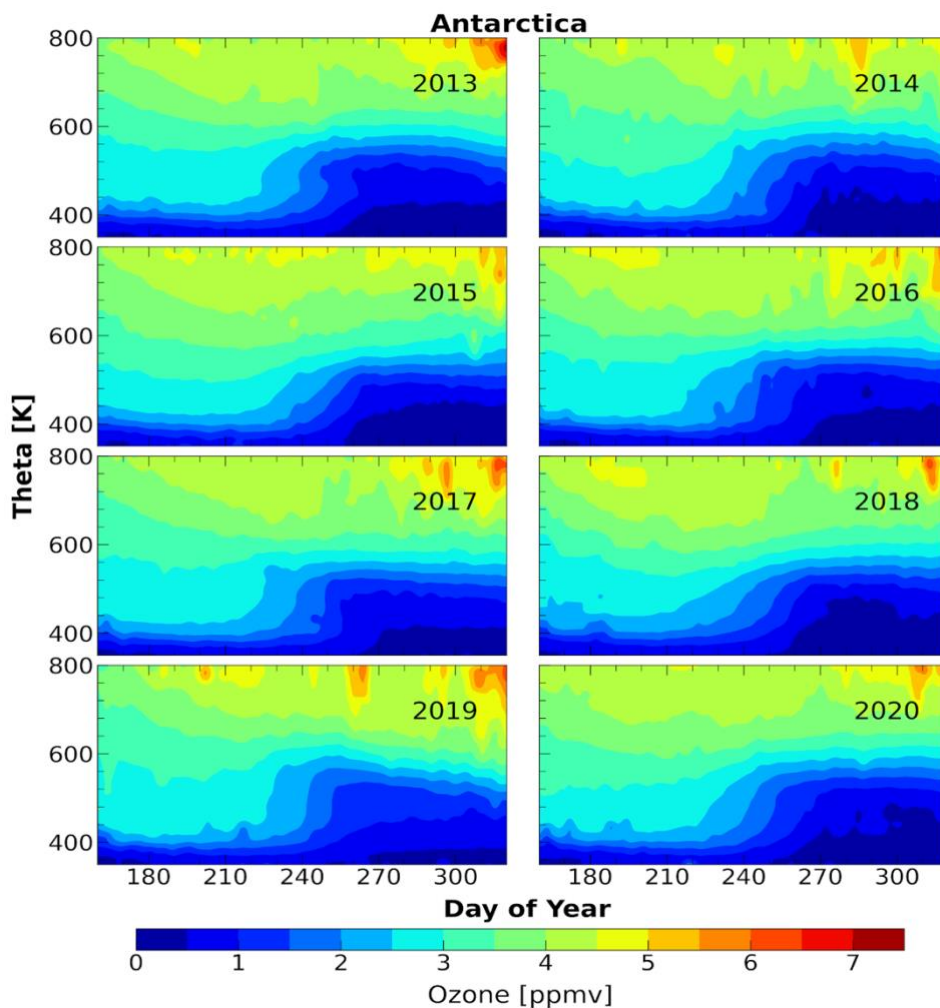
295

296

297

298

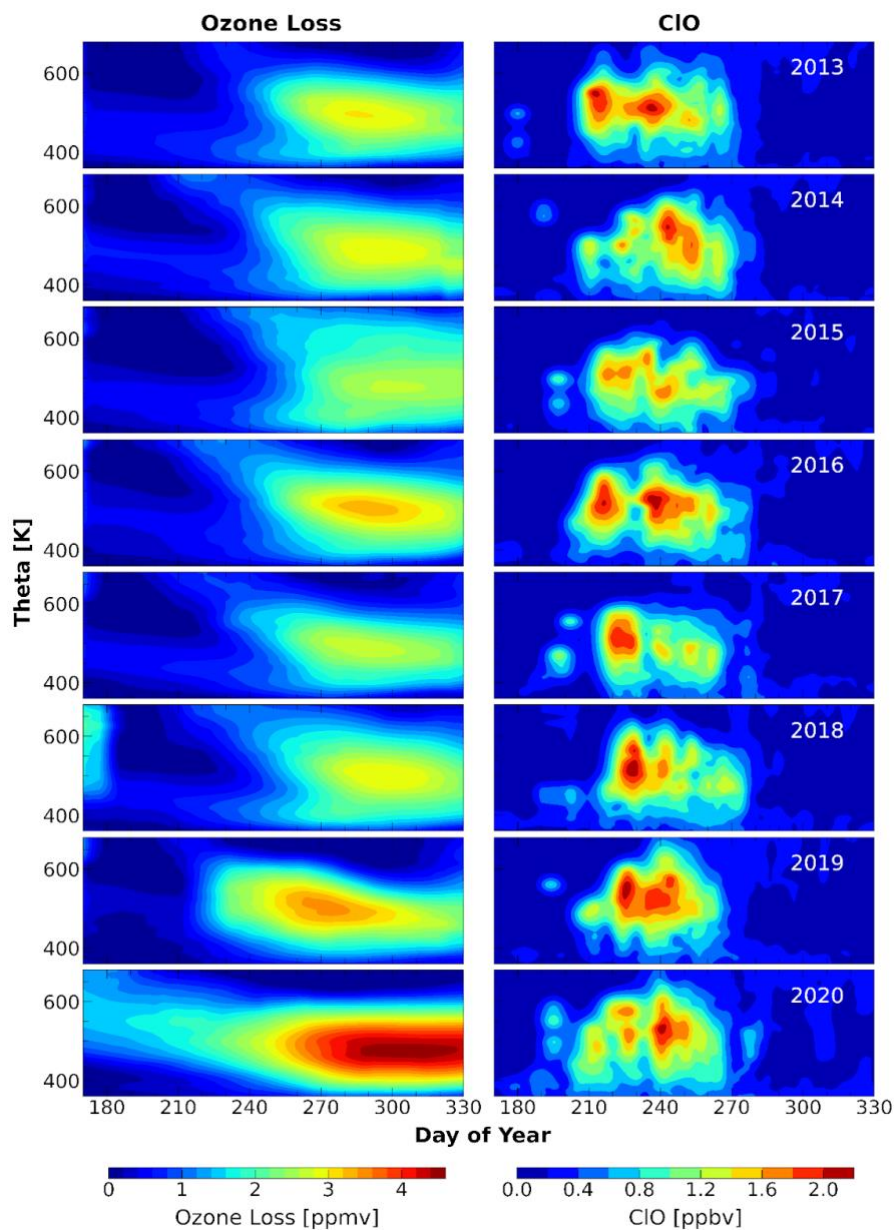
Figure 2: Seasonal march of the zonal mean temperature for the period 2003–2020 averaged over the latitudes 60–90°S. The contours show the temperature and the white contours represent specific temperatures such as 188, 195 and 210 K. The zonal wind velocities are overlaid. The black contour lines show the westerlies and the red contour lines show the easterlies.



299
300

301 **Figure 3:** Temporal evolution of the vertical profiles of ozone averaged inside the vortex for the winters from
302 2013 to 2020 in the Antarctic. MLS data are used for the estimation. The temporal evolution is analysed for the
303 period June–November and for the altitude range 350–800 K.

304



305

306

307

308

309

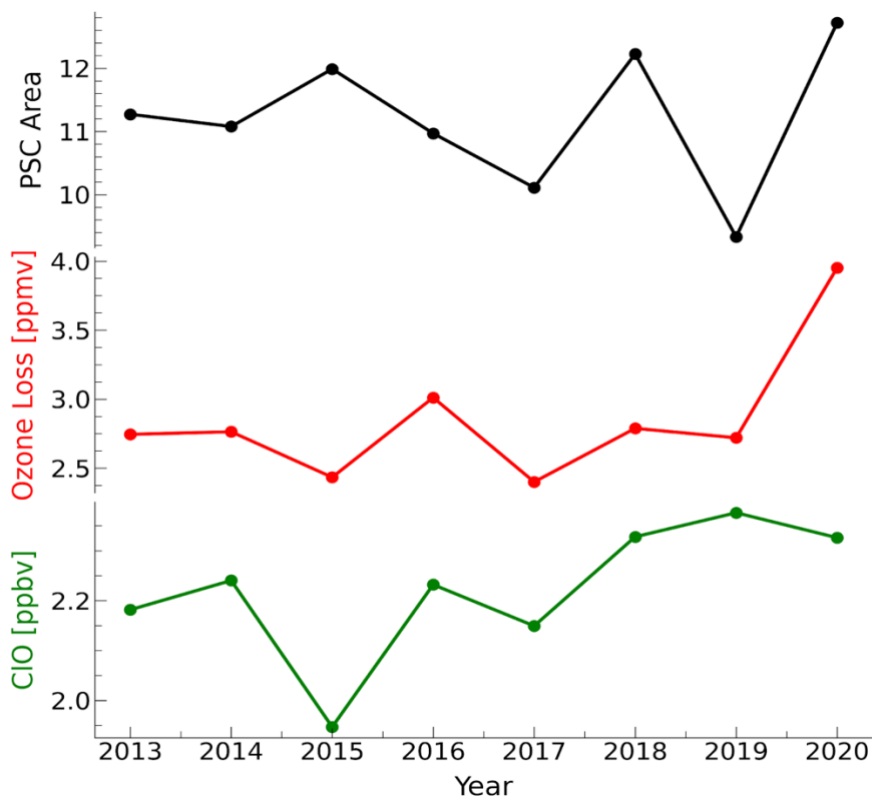
Figure 4: Temporal evolution of ozone loss estimated from MLS measurements using REPROBUS passive tracer (left). The MLS CIO measurements for the altitude range 350–700 K for the period 2013–2020. The ozone loss estimates and CIO measurements are selected inside the polar vortex as per the Nash et al. (1996) criterion.



310

311

312



313

314

315 **Figure 5:** The vortex-averaged ozone loss estimated from the MLS measurements using the passive method, peak
316 ClO measurements, and the weighted average of area of PSC for the period 2013–2020. The mean ozone loss is
317 estimated over the altitude range 450–550 K for the day 270 and day 300 (maximum ozone loss days). The ClO
318 measurements are averaged over the altitude range 450–550 K and for the day 210 and day 270; representing the
319 strong chlorine activation period and altitudes.

320

321

322

323



324 **REFERENCES**

- 325 Angell, J. K. and Free, M.: Ground-based observations of the slowdown in ozone decline and onset of ozone
326 increase, *J. Geophys. Res.*, 114, D07303, doi:10.1029/2008JD010860, 2009.
- 327 Bandoro, J., Solomon, S., Donohoe, A., Thompson, D.W.J., and Santer, B.D.: Influences of the Antarctic ozone
328 hole on Southern Hemispheric summer climate change. *Journal of Climate*. 27(16):6245–6264. doi:
329 10.1175/JCLI-D-13-00698.1, 2014.
- 330 Braathen, G. O.: Observations of the Antarctic Ozone Hole from 2003 to 2017, p. 16503, 2018.
- 331 Butler, A., Daniel, J. S., Portmann, R. W., Ravishankara, A., Young, P. J., Fahey, D. W., and Rosenlof, K. H.:
332 Diverse policy implications for future ozone and surface UV in a changing climate, *Environ. Res. Lett.*, 11,
333 064 017, <https://doi.org/10.1088/1748-9326/11/6/064017>, 2016.
- 334 Chipperfield, M. P., Bekki, S., Dhomse, S., Harris, N. R., Hassler, B., Hossaini, R., Steinbrecht, W.,
335 Thiéblemont, R., and Weber, M.: Detecting recovery of the stratospheric ozone layer, *Nature*, 549, 211,
336 <https://doi.org/10.1038/nature23681>, 2017.
- 337 Damiani, A., Cordero, R. R., Llanillo, P. J., Feron, S., Boisier, J. P., Garreaud, R., Rondanelli, R., Irie, H., and
338 Watanabe, S.: Connection between antarctic ozone and climate: Interannual precipitation changes in the Southern
339 Hemisphere. *Atmosphere*, 11(6), 1–19. <https://doi.org/10.3390/atmos11060579>, 2020.
- 340 de Laat, A. T. J., van Weele, M., and van der A, R. J.: Onset of stratospheric ozone recovery in the Antarctic
341 ozone hole in assimilated daily total ozone columns, *J. Geophys. Res.-Atmos.*, 122, 11880–11899,
342 <https://doi.org/10.1002/2016JD025723>, 2017.
- 343 Dee, D. P., Uppala, S. M., Simmons, A. J., Berrisford, P., Poli, P., Kobayashi, S., Andrae, U., Balmaseda, M. A.,
344 Balsamo, G., Bauer, P., Bechtold, P., Beljaars, A. C. M., van de Berg, L., Bidlot, J., Bormann, N., Delsol, C.,
345 Dragani, R., Fuentes, M., Geer, A. J., Haimberger, L., Healy S. B., Hersbach, H., Hólm E. V., Isaksen,
346 L., Kållberg, P., Köhler, M., Matricardi, M., McNally, A. P., Monge-Sanz, B. M., Morcrette J.-J., Park B.-K.,
347 Peubey, C., de Rosnay, P., Tavolato, C., Thépaut J.-N., and Vitart, F.: The ERA-Interim reanalysis: configuration
348 and performance of the data assimilation system. *Q. J. R. Meteorol. Soc.*, 137, 553–597.
349 <https://doi.org/10.1002/qj.828>, 2011.
- 350 Dhomse, S. S., Feng, W., Montzka, S. A., Hossaini, R., Keeble, J., Pyle, J. A., Daniel, J. S., and Chipperfield, M.
351 P.: Delay in recovery of the Antarctic ozone hole from unexpected CFC-11
352 emissions. *Nature Communications*, 10(1), 1–12. <https://doi.org/10.1038/s41467-019-13717-x>, 2019.
- 353 Evtushevsky, O. M., Klekociuk, A. R., Kravchenko, V. O., Milinevsky, G. P., and Grytsai, A. V.: The influence
354 of large amplitude planetary waves on the Antarctic ozone hole of austral spring 2017. *J. South. Hemisph. Earth
355 Syst. Sci.* 69, 57–64. doi:10.1071/ES19022, 2019.
- 356 Farman, J. C., B. G. Gardiner, and J. D. Shanklin.: Large losses of total ozone in Antarctica reveal seasonal
357 ClOx/NOx interaction, *Nature*, 315, 207-210, 1985.



- 358 Froidevaux, L., Jiang, Y. B., Lambert, A., Livesey, N. J., Read, W. G.; Waters, J. W., Browell, E. V., Hair, J. W.,
359 Avery, M. A., McGee, T. J., Twigg, L. W., Sumnicht, G. K., Jucks, K. W., Margitan, J. J., Sen, B., Stachnik, R.
360 A., Toon, G. C., Bernath, P. F., Boone, C. D., Walker, K. A., Filipiak, M. J., Harwood, R. S., Fuller, R. A.,
361 Manney, G. L., Schwartz, M. J., Daffer, W. H., Drouin, B. J., Cofield, R. E., Cuddy, D. T., Jarnot, R. F., Knosp,
362 B. W., Perun, V. S., Snyder, W. V., Stek, P. C., Thurstans, R. P., and Wagner, P. A.: Validation of Aura
363 Microwave Limb Sounder stratospheric ozone measurements. *Journal of Geophysical Research*, 113(D15),
364 D15S20–. doi:10.1029/2007jd008771, 2008
- 365 Gelaro, R., McCarty, W., Suárez, M. J., Todling, R., Molod, A., Takacs, L., Randles, C. A., Darmenov, A.,
366 Bosilovich, M. G., Reichle, R., Wargan, K., Coy, L., Cullather, R., Draper, C., Akella, S., Buchard, V., Conaty,
367 A., da Silva, A. M., Gu, W., Kim, G.-K., Koster, R., Lucchesi, R., Merkova, D., Nielsen, J. E., Partyka, G.,
368 Pawson, S., Putman, W., Rienecker, M., Schubert, S. D., Sienkiewicz, M., and Zhao, B.: The Modern-Era
369 Retrospective Analysis for Research and Applications, Version 2 (MERRA-2), *J. Climate*, 30, 5419–5454,
370 <https://doi.org/10.1175/JCLI-D-16-0758.1>, 2017.
- 371 Klekociuk, A. R., Tully, M. B., Alexander, S. P., Dargaville, R. J., Deschamps, L. L., Fraser, P. J., Gies, H. P.,
372 Henderson, S. I., Javorniczky, J., Krummel, P. B., Petelina, S. V., Shanklin, J. D., Siddaway, J. M., and Stone, K.
373 A.: The Antarctic ozone hole during 2010. *Australian Meteorological and Oceanographic Journal*, 61(4), 253–
374 267. <https://doi.org/10.22499/2.6104.006>, 2015.
- 375 Krummel, P. B., Fraser, P. J., and Derek, N.: The 2015 Antarctic ozone hole and ozone science summary: final
376 report. (Report prepared for the Australian Government Department of the Environment, CSIRO:Australia.) iv,
377 27 pp, 2016.
- 378 Kuttippurath, J., Kumar, P., Nair, P. J., and Pandey, P. C.: Emergence of ozone recovery evidenced by reduction
379 in the occurrence of Antarctic ozone loss saturation. *Npj Climate and Atmospheric Science*, 1(1).
380 doi:10.1038/s41612-018-0052-6, 2018.
- 381 Kuttippurath, J., and Nair, P. J.: The signs of Antarctic ozone hole recovery. *Sci. Rep.*, 7, 585,
382 doi:10.1038/s41598-017-00722-7, 2017.
- 383 Kuttippurath, J., Godin-Beekmann, S., Lefèvre, F., Santee, M. L., Froidevaux, L., and Hauchecorne, A.:
384 Variability in Antarctic ozone loss in the last decade(2004–2013): high-resolution simulations compared to Aura
385 MLS observations, *Atmos. Chem. Phys.*, 15, 10385–10397, <https://doi.org/10.5194/acp-15-10385-2015>, 2015.
- 386 Langematz, U., and Kunze, M.: An update on dynamical changes in the Arctic and Antarctic stratospheric polar
387 vortices. *Clim Dyn* 27, 647–660. <https://doi.org/10.1007/s00382-006-0156-2>, 2006.
- 388 Lefèvre, F., Brasseur, G. P., Folkins, I., Smith, A. K., and Simon, P.: Chemistry of the 1991/1992 stratospheric
389 winter: three-dimensional model simulation, *J. Geophys. Res.*, 99, 8183–8195, 1994.
- 390 Livesey, N. J., Read, W. G., Froidevaux, L., Lambert, A., Manney, G. L., Pumphrey, H. C., Santee, M. L.,
391 Schwartz, M. J., Wang, S., Cofield, R. E., Cuddy, D. T., Fuller, R. A., Jarnot, R. F., Jiang, J. H., Knosp, B. W.,
392 Stek, P. C., Wagner, P. A., and Wu, D. L.: Earth Observing System (EOS) Aura Microwave Limb Sounder
393 (MLS) Version 3.3 and 3.4 Level 2 data quality and description document, JPL D-33509, Jet Propulsion
394 Laboratory California Institute of Technology, Pasadena, California, USA, 1–164, 2013.



- 395 Maione, M., Graziosi, F., Arduini, J., Furlani, F., Giostra, U., Blake, D. R., Bonasoni, P., Fang, X., Montzka, S.
396 A., O'Doherty, S. J., Reimann, S., Stohl, A., and Vollmer, M. K.: Estimates of European emissions of methyl
397 chloroform using a Bayesian inversion method, *Atmos. Chem. Phys.*, 14, 9755–9770,
398 <https://doi.org/10.5194/acp-14-9755-2014>, 2014.
- 399 Maliniemi, V., Nesse Tyssøy, H., Smith-Johnsen, C., Arsenovic, P., and Marsh, D.: Ozone super recovery
400 cancelled in the Antarctic upper stratosphere. *Atmospheric Chemistry and Physics*, February, 1–15.
401 <https://doi.org/10.5194/acp-2021-149>, 2021
- 402 Milinevsky, G., Evtushevsky, O., Klekociuk, A., Wang, Y., Grytsai, A., Shulga, V., and Ivaniha, O.: Early
403 indications of anomalous behaviour in the 2019 spring ozone hole over Antarctica. *International Journal of*
404 *Remote Sensing*, 41(19), 7530–7540. <https://doi.org/10.1080/2150704X.2020.1763497>, 2020.
- 405 Montzka, S. A., G. S. Dutton, P. Yu, E. Ray, R. W. Portmann, J. S. Daniel, L. Kuijpers, B.
406 D. Hall, D. Mondeel, C. Siso, J. D. Nance, M. Rigby A. J. Manning, L. Hu, F. Moore, B. R. Miller,
407 and J. W. Elkins.: An unexpected and persistent increase in global emissions of ozone-depleting CFC-11.
408 *Nature*, 557, 413-417, 2018.
- 409 Müller, R., Tilmes, S., Konopka, P., Groß, J.-U., and Jost, H.-J.: Impact of mixing and chemical change on
410 ozone-tracer relations in the polar vortex, *Atmos. Chem. Phys.*, 5, 3139–3151, [https://doi.org/10.5194/acp-5-](https://doi.org/10.5194/acp-5-3139-2005)
411 [3139-2005](https://doi.org/10.5194/acp-5-3139-2005), 2005.
- 412 Nash, E. R., Newman, P. A., Rosenfield, J. E., and Schoeberl, M. R.: An objective determination of the polar
413 vortex using Ertel's potential vorticity, *J. Geophys. Res.*, 101, 9471–9478, 1996.
- 414 Nedoluha, G. E., Connor, B. J., Mooney, T., Barrett, J. W., Parrish, A., Gomez, R. M., Boyd, I., Allen, D. R.,
415 Kotkamp, M., Kremser, S., Deshler, T., Newman, P., and Santee, M. L.: 20 years of ClO measurements in the
416 Antarctic lower stratosphere. *Atmos. Chem. Phys.*, 16(16), 10725–10734. [https://doi.org/10.5194/acp-16-10725-](https://doi.org/10.5194/acp-16-10725-2016)
417 [2016](https://doi.org/10.5194/acp-16-10725-2016), 2016.
- 418 Pazmiño, A., S. Godin-
419 Beekmann, A. Hauchecorne, C. Claud, S. Khaykin, F. Goutail, E. Wolfram, J. Salvador, and E. Quel.:
420 Multiple symptoms of total ozone recovery inside the Antarctic vortex during austral spring. *Atmos. Chem.*
421 *Phys.*, 18, 7557-7572, 2018.
- 422 Polvani, L. M., Previdi, M., England, M. R., Chiodo, G., and Smith, K. L.: Substantial twentieth-century Arctic
423 warming caused by ozone-depleting substances. *Nature Climate Change*, 10(2), 130–133.
424 <https://doi.org/10.1038/s41558-019-0677-4>, 2020.
- 425 Rigby, M., Montzka, S. A., Prinn, R. G., White, J. W. C., Young, D., O'Doherty, S., Lunt, M. F., Ganesan, A. L.,
426 Manning, A. J., Simmonds, P. G., Salameh, P. K., Harth, C. M., Mühle, J., Weiss, R. F., Fraser, P. J., Steele, L.
427 P., Krummel, P. B., McCulloch, A., and Park, S.: Role of atmospheric oxidation in recent methane growth.
428 *Proceedings of the National Academy of Sciences of the United States of America*, 114(21), 5373–5377.
429 <https://doi.org/10.1073/pnas.1616426114>, 2017



- 430 Rowland, F. S., J. E. Spencer, and M. J. Molina.: Stratospheric formation and photolysis of chlorine nitrate, J.
431 Phys. Chem., 80, 2711-2713, 1976.
- 432 Roy, R., Kuttippurath, J., Lefèvre, F. et al. The sudden stratospheric warming and chemical ozone loss
433 in the Antarctic winter 2019: comparison with the winters of 1988 and 2002. *Theor Appl Climatol* 149,
434 119–130. <https://doi.org/10.1007/s00704-022-04031-6>, 2022
- 435 Salby, M., E. Titova, and L. Deschamps.: Rebound of Antarctic ozone. *Geophys. Res. Lett.*, 38, L09702,
436 doi:10.1029/2011GL047266, 2011.
- 437 Santee, M., MacKenzie, I. A., Manney, G., Chipperfield, M., Bernath, P. F., Walker, K. A., Boone, C. D.,
438 Froidevaux, L., Livesey, N., and Waters, J. W.: A study of stratospheric chlorine partitioning based on new
439 satellite measurements and modeling, *J. Geophys. Res.*, 113, D12307, doi:10.1029/2007JD009057, 2008.
- 440 Shen, X., Wang, L., and Osprey, S.: Tropospheric forcing of the 2019 Antarctic sudden stratospheric warming.
441 *Geophysical Research Letters*, 47, e2020GL089343. <https://doi.org/10.1029/2020GL089343>, 2020b.
- 442 Shen, X., Wang, L., and Osprey, S.: The Southern Hemisphere sudden stratospheric warming of September 2019.
443 *Science Bulletin*. doi:10.1016/j.scib.2020.06.028, 2020.
- 444 Solomon, S., Ivy, D. J., Kinnison, D., Mills, M. J., Neely, R. R. III, and Schmidt, A.: Emergence of healing in the
445 Antarctic ozone layer. *Science*, 252(6296), 269–274. <https://doi.org/10.1126/science.aae006>, 2016.
- 446 Solomon, S.: Stratospheric ozone depletion: A review of concepts and history. *Reviews of Geophysics*, 37(3),
447 275–316. doi:10.1029/1999rg900008, 1999.
- 448 Solomon, S., Haskins, J., Ivy, D. J., Min, F.: Fundamental differences between Arctic and Antarctic ozone
449 depletion. *Proceedings of the National Academy of Sciences*, 111(17), 6220–6225.
450 doi:10.1073/pnas.1319307111, 2014.
- 451 SPARC: Liang, Q., Newman P. A., Reimann, S. (Eds.), Report on the Mystery of Carbon Tetrachloride
452 (SPARC Report No. 7 WCRP-13/2016) (2016).
- 453 Stolarski, R. S., and R. J. Cicerone.: Stratospheric chlorine: A possible sink for ozone, *Can. J. Chem.*, 52, 1610-
454 1615, 1974.
- 455 Stolarski, R. S., Douglass, A. R., Gupta, M., Newman, P. A., Pawson, S., Schoeberl, M. R., and Nielsen, J. E.: An
456 ozone increase in the Antarctic summer stratosphere: A dynamical response to the ozone hole, *Geophys. Res.*
457 *Lett.*, 33, L21805, doi:10.1029/2006GL026820, 2006.
- 458 Stone, K. A., Solomon, S., Kinnison, D. E., and Mills, M. J.: On recent large Antarctic ozone holes and ozone
459 recovery metrics. *Geophysical Research Letters*, 48, e2021GL095232. <https://doi.org/10.1029/2021GL095232>,
460 2021.



- 461 Strahan, S. E., and Douglass, A. R.: Decline in Antarctic ozone depletion and lower stratospheric chlorine
462 determined from Aura Microwave Limb Sounder observations. *Geophysical Research Letters*, 45, 382– 390.
463 <https://doi.org/10.1002/2017GL074830>, 2018.
- 464 Strahan, S. E., Douglass, A. R., Newman, P. A., and Steenrod, S. D.: Inorganic chlorine variability in the
465 Antarctic vortex and implications for ozone recovery. *Journal of Geophysical Research: Atmospheres*, 119,
466 14,098– 14,109, 2014.
- 467 Tully, M. B., Klekociuk, A. R., Krummel, P. B., Gies, H. P., Alexander, S. P., Fraser, P. J., Henderson, S. I.,
468 Schofield, R., Shanklin, J. D., and Stone, K. A.: The Antarctic ozone hole during 2015 and 2016. *Journal of*
469 *Southern Hemisphere Earth Systems Science*, 69(1), 16. <https://doi.org/10.1071/es19021>, 2019.
- 470 Vargin, P.N., Nikiforova, M.P. and Zvyagintsev, A.M.: Variability of the Antarctic Ozone Anomaly in 2011–
471 2018. *Russ. Meteorol. Hydrol.* 45, 63–73. <https://doi.org/10.3103/S1068373920020016>, 2020.
- 472 Wargan, K., Weir, B., Manney, G. L., Cohn, S. E., and Livesey, N. J.: The anomalous 2019 Antarctic ozone hole
473 in the GEOS Constituent Data Assimilation System with MLS observations. *Journal of Geophysical Research:*
474 *Atmospheres*, 125, e2020JD033335. <https://doi.org/10.1029/2020JD033335>, 2020.
- 475 Weatherhead, E. C., Reinsel, G. C., Tiao, G. C., Jackman, C. H., Bishop, L., Hollandsworth Frith, S. M., DeLuisi,
476 J., Keller, T., Oltmans, S. J., Fleming, E. L., Wuebbles, D. J., Kerr, J. B., Miller, A. J., Herman, J., McPeters, R.,
477 Nagatani, R. M., and Frederick, J. E.: Detecting the recovery of total column ozone. *Journal of Geophysical*
478 *Research-Atmospheres*, 105(D17), 22201–22210. <https://doi.org/10.1029/2000JD900063>, 2000.
- 479 Wespes, C., Hurtmans, D., Chabrillat, S., Ronsmans, G., Clerbaux, C., and Coheur, P.-F.: Is the recovery of
480 stratospheric O₃ speeding up in the Southern Hemisphere? An evaluation from the first IASI decadal record
481 (2008–2017), *Atmos. Chem. Phys.*, 19, 14031–14056, <https://doi.org/10.5194/acp-19-14031-2019>, 2019.
- 482 Wigley, T.: Future CFC concentrations under the Montreal Protocol and their greenhouse-effect implications.
483 *Nature* 335, 333–335. <https://doi.org/10.1038/335333a0>, 1988.
- 484 Williamson, D. L. and Rasch, P. J.: Two-dimensional semi-Lagrangian transport with shape-preserving
485 interpolation, *Mon. Weather Rev.*, 117, 102–129, 1989.
- 486 WMO (World Meteorological Organization): Scientific Assessment of Ozone Depletion: 2006, Global Ozone
487 Research and Monitoring Project – Report No. 50, 572 pp., Geneva, 2007
- 488 WMO: Scientific Assessment of Ozone Depletion: 2014 Global Ozone Research and Monitoring Project Report,
489 World Meteorological Organization, Geneva, Switzerland, p. 416, 2014.
- 490 World Meteorological Organization (WMO) (2015), WMO Antarctic Ozone Bulletins (2015). [Available at
491 www.wmo.int/pages/prog/arep/WMOAntarcticOzoneBulletins2015.html.]
- 492 Yamazaki, Y., Matthias, V., Miyoshi, Y., Stolle, C., Siddiqui, T., Kervalishvili, G., LaÅ;toiviÄka, J., Kozubek,
493 M., Ward, W., Themens, D. R., Kristoffersen, S., Alken, P.: September 2019 Antarctic Sudden Stratospheric



- 494 Warming: Quasi-Daily Wave Burst and Ionospheric Effects. *Geophysical Research Letters*, 47(1), –.
495 doi:10.1029/2019GL086577, 2020.
- 496 Yang, E.-S., Cunnold, D. M., Newchurch, M. J., Salawitch, R. J., McCormick, M. P., Russell, J. M., Zawodny, J.
497 M., and Oltmans, S. J.: First stage of Antarctic ozone recovery, *J. Geophys. Res.*, 113, D20308,
498 <https://doi.org/10.1029/2007JD009675>, 2008.
- 499 Zhang, Y., Li, J., and Zhou, L.: The Relationship between Polar Vortex and Ozone Depletion in the Antarctic
500 Stratosphere during the Period 1979–2016. *Advances in Meteorology*, 2017, 1–12. doi:10.1155/2017/3078079,
501 2017.
- 502 Zuev, V. V., and Savelieva, E.: The cause of the spring strengthening of the Antarctic polar vortex. *Dynamics of*
503 *Atmospheres and Oceans*, 87, 101097. doi:10.1016/j.dynatmoce.2019.101097, 2019.
- 504
- 505
- 506
- 507
- 508
- 509 V08/JK/04112021
- 510
- 511